ECOHYDROLOGY
Ecohydrol. (2016)
Published online in Wiley Online Library
(wileyonlinelibrary.com) DOI: 10.1002/eco.1748

Attribution of the vegetation trends in a typical desertified watershed of northeast China over the past three decades

Siru Wang,[1,2] Huimin Lei,[1]* Limin Duan,[3] Tingxi Liu[3] and Dawen Yang[1]

[1] *State Key Laboratory of Hydroscience and Engineering, Department of Hydraulic Engineering, Tsinghua University, Beijing 100084, China*
[2] *State Key Laboratory of Hydrology and Water Resources and Hydraulic Engineering Science, Nanjing Hydraulic Research Institute, Nanjing 210029, China*
[3] *College of Conservancy and Civil Engineering, Inner Mongolia Agricultural University, Hohhot 010018, China*

ABSTRACT

Desertification is a serious environmental problem in north China that should be urgently addressed and prevented. Identifying the causes of vegetation trends that are closely related to desertification is prerequisite for a better control of desertification processes. In this study, the Xiliao River basin, a typical desertified watershed in northeast China, was selected as a case study. To partition the vegetation trends into climate-induced and human-induced trends, a linear regression model, piecewise regression model and a binary nonlinear regression analysis were employed, based on the long-term remote measures of the Normalized Difference Vegetation Index (NDVI) and climate data. The results showed that the spatial pattern of the vegetation trends in the basin was highly heterogonous, although the climatic factors varied similarly. In the north, where natural vegetation dominates, the vegetation exhibited significant browning ($-0.0015\,\text{year}^{-1}$), and a significant changing point was observed in 2000. In the south, where cropland dominates, the vegetation exhibited significant greening ($0.002\,\text{year}^{-1}$). Approximately 82.7% of the area with a decreasing NDVI was attributed to climate variability. The main reason for the vegetation degradation was because of a multiyear reduction in precipitation from 1999 to 2011 rather than from an increase in the grazing size. Approximately 67.0% of the area with an increasing NDVI could be attributed to irrigation, which overexploited a large amount of water resources, even though significantly increasing air temperatures can promote vegetation greenness. Our findings have important management implications for grazing and agriculture in the context of controlling desertification and sustaining environment. Copyright © 2016 John Wiley & Sons, Ltd.

KEY WORDS vegetation change; attribution analysis; binary nonlinear regression; desertified watershed; north China

Received 20 July 2015; Revised 28 April 2016; Accepted 1 May 2016

INTRODUCTION

Desertification is characterized as a long-term decline in the functions and productivity of an ecosystem, which are mainly related to vegetation growth. It has serious implications for eco-safety, food security, socio-economic stability and sustainable development (Reynolds *et al*., 2007). Vegetation growth is determined by both climate variability and human activities. Among these factors, air temperature and precipitation are the key climatic factors that directly affect vegetation through photosynthesis and soil moisture stress, respectively (Goetz *et al*., 2005; Piao *et al*., 2006). As shown by previous studies, increasing air temperature has already promoted vegetation growth, as indicated by the vegetation greening throughout much of the Northern Hemisphere (Zhou *et al*., 2001; Jia *et al*., 2009), and drought because of the reduction in precipitation caused vegetation browning in global terrestrial areas during 2000–2009 (Zhao and Running, 2010). Human activities, such as overgrazing, mowing and urbanization, are considered to have negative effects on vegetation growth (Runnström, 2000; Sheng *et al*., 2000), while afforestation has positive effects on vegetation dynamics (Tilman, 1999). The effects of the conversion of natural land to cropland are relatively uncertain because they depend on the relationship between cropland management (e.g. fertilization and irrigation) and the vegetation growth status in the natural land. Although both climate and human activities have huge impacts on vegetation growth, previous studies about the large-scale changes in vegetation primarily focused on the effects of climatic factors and usually failed to consider the effects of human activities, such as cropland management and grazing (e.g. Piao *et al*., 2015; Wu *et al*., 2015). Thus, considering the complex impacts of climate and human activities on vegetation growth, a prerequisite for obtaining a better understanding

*Correspondence to: Huimin Lei, Department of Hydraulic Engineering, Tsinghua University, Beijing 100084, China. E-mail leihm@tsinghua.edu.cn

of the desertification processes is to attribute the trends in vegetation to the effects of climate and human activities.

The Xiliao River basin is a desertified basin located in northeast China (also in the Inner Mongolian Steppe), and includes a famous desertified region known as the Horqin Sandy land (Figure 1). It is an agro-pastoral transition zone, and there is an intense conflict between human beings and nature for its water and land resources. Over the past three decades, a significant decreasing trend in vegetation was observed around this basin, even though overall greening trends have been detected in most regions of China (Peng *et al*., 2011; Piao *et al*., 2015). Thus, a comprehensive understanding of the characteristics of vegetation degradation and its driving factors is essential for desertification control in this region.

In general, overgrazing is considered to be one of the important causes of desertification in semi-arid and arid zones, such as the Mongolian Steppe and Inner Mongolian Steppe, while the primary contributor (i.e. climate, overgrazing or both) to the degradation of the steppe is still in debate. For example, Liu *et al*. (2013) concluded that approximately 60% of the decrease in vegetation can be attributed to the climate trends in the Mongolian Steppe during 1998–2008; however, Hilker *et al*. (2014) reported that approximately 80% of the decrease in the Normalized Difference Vegetation Index (NDVI) could be attributed to

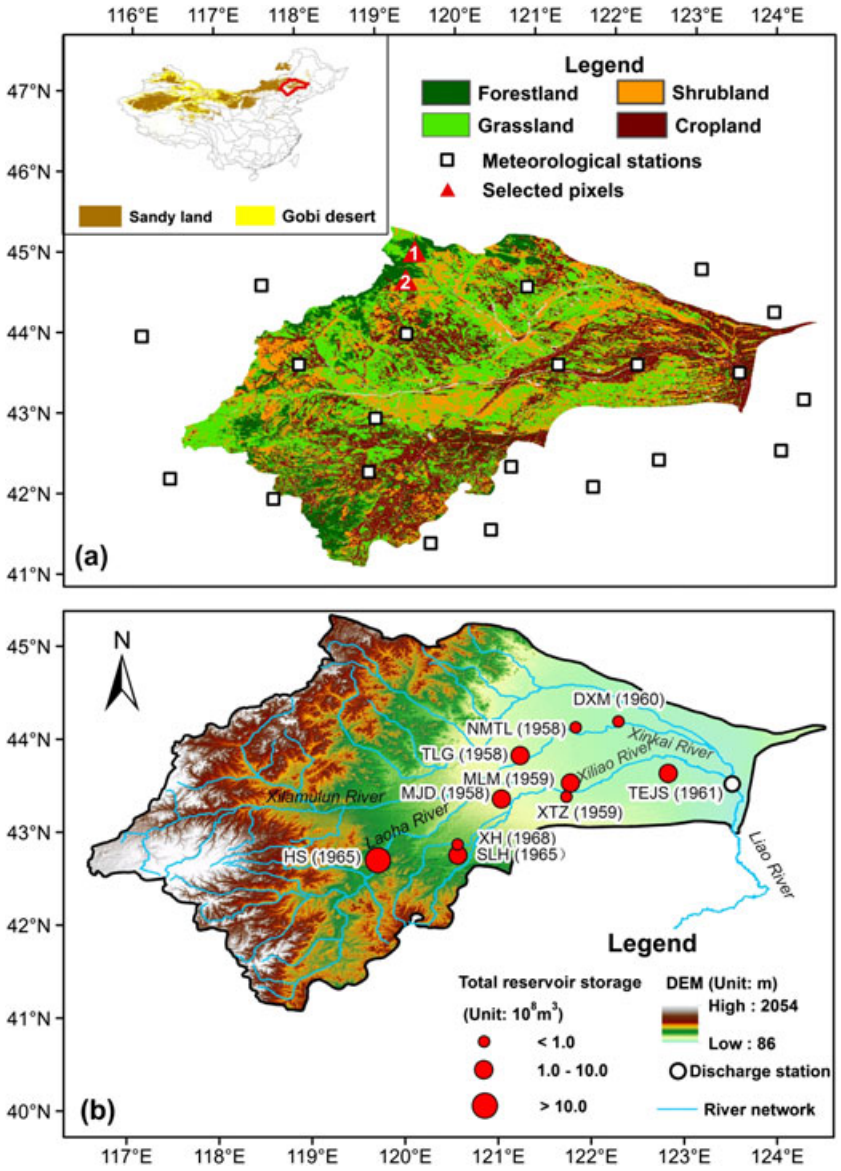

Figure 1. (a) Location of the Xiliao River basin and (b) geographical information for this basin. The upper left desertification map in Figure 1(a)) was generated by the Cold and Arid Regions Environmental and Engineering Research Institute, Chinese Academy of Sciences. The criteria for the desertification area are based on the sand particle percentage (between 79% and 99%), organic content (between 0.065% and 0.975%) and its roughness (between 0.001 and 2.33). The two red triangles are the pixels that were selected to evaluate the regression model.

an increase in the number of livestock in the same region during 2002–2012. Moreover, the role of cropland in the changes in vegetation greenness is not clear. For example, Guo *et al*. (2014) indicated that an increase in the NDVI benefitted from cropland management in Inner Mongolia, while Mu *et al*. (2013) suggested that the large-scale conversion of grassland to cropland contributed to a decrease in the net primary productivity, which is closely related to the NDVI. The obvious differences in the results from these studies can be attributed to the different study periods, datasets or methods, indicating that it is still necessary to explore whether the overall decreasing vegetation trend in the Xiliao River basin was climate induced. However, to our knowledge, there has been no quantitative analysis aimed at attributing the vegetation degradation, although some studies have already qualitatively explored the responses of vegetation dynamics to climate in large regions including this basin (Piao *et al*., 2005; Piao *et al*., 2006; Bao *et al*., 2014; Guo *et al*., 2014).

The objectives of this study are to investigate the satellite-observed vegetation trends in the Xiliao River basin over the past three decades and quantitatively identify the attribution of the vegetation trends (climate dominated or human dominated). In this study, a simple empirical model was employed to quantitatively partition the vegetation trends in a watershed that facilitates investigations into the variations in water consumption in a region, which is different from previous studies that show separate trends in the climatic factors and NDVI in the temperate steppe (Piao *et al*., 2006; Mu *et al*., 2013). First, to identify the general changes in precipitation, temperature and the NDVI during the average growing period (from April to October) over the past three decades, we used linear and piecewise regression models to test the trend and change point in the time series, respectively (Toms and Lesperance, 2003; Piao *et al*., 2005). Then, we employed a binary nonlinear regression model to attribute the vegetation trends. Finally, we discussed the possible connections between human activities and the vegetation trends.

STUDY AREA

The Xiliao River basin lies within 41.2–45.4°N and 116.6–124.5°E, and has a drainage area of approximately 0.14 million km^2. It consists of a large amount of desertified sandy land and is identified as a desertification area (the upper left map in Figure 1(a)). The major stream is primarily located in the south plain terrain, where several large reservoirs were established (Figure 1(b)). The basin belongs to the continental monsoon climate zone and has a semi-arid climate. The annual cumulative precipitation and mean temperature from 1982 to 2011 were 388 mm and 6 °C, respectively. Figure 2 shows the spatial distribution of the average annual NDVI, precipitation and temperature over the basin, as well as the seasonal cycle of the basin-average NDVI, precipitation and temperature. The average annual NDVI in more than 62% of the basin is less than 0.30, which is low compared with other well-growth

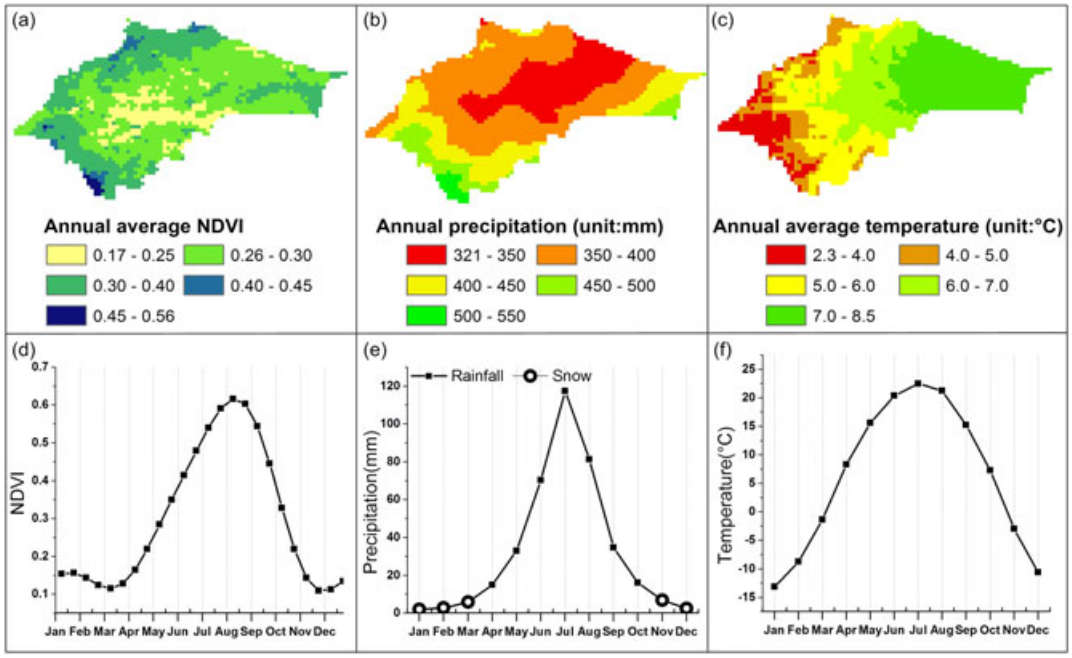

Figure 2. Average annual (a) NDVI, (b) precipitation and (c) temperature over the basin. Seasonal cycle of the basin-average (d) NDVI, (e) precipitation and (f) temperature. The snow data were separated from the rainfall data using air temperatures of 3–3.5 °C (Han *et al*., 2010).

vegetation (the average NDVI of the growing season is approximately 0.62 (Liu *et al.*, 2015)), and is similar with other desertification areas, such as the Mongolian Steppes, where the average annual NDVI in the barren and grasslands is generally between 0.1 and 0.4 (Liu *et al.*, 2013). The NDVI reached its peak in the first half of August, and the precipitation and air temperature reached their peaks in July. The snow events occurred during the non-growing period (November to March) for the vegetation, and the amount of snow was quite small. The basin is a typical farming-pastoral zone in north China. Farming and stockbreeding are the two most important sectors in agriculture. The total number of livestock (21 020 000 in 2011) has nearly doubled, and the crop yield (10.4 million tons in 2011) has increased nearly threefold over the past two decades. The primary livestock are cattle and sheep/goats (the ratio of cattle to sheep/goats is 4:11). According to the land use map in 2010 (Figure 1(a)), the main land use types were grassland (37%), cropland (31%), shrubland (19%) and forestland (13%). Cropland is mainly distributed in the plain area and valley of the basin (Figure 1(a–b)), and the distribution of livestock is relatively homogeneous. The diverse land use types in this basin provide us a good opportunity to comparatively analyse the impacts of climate change, grazing and cropland management on vegetation trends in the same framework compared to the relatively homogenous landscape used in previous studies (Liu *et al.*, 2013).

MATERIALS AND METHODS

Data acquisition and processing

The NDVI is a measure of the chlorophyll abundance in the leaves (Myneni *et al.*, 1995). It is an indicator of vegetation coverage and greenness, and has already been widely used to analyse trends in vegetation (Kawabata *et al.*, 2001; Piao *et al.*, 2011). The average NDVI during a period represents the average vegetation growth state, which is a consequence of the effects of climatic and anthropogenic factors during and/or before this period. In this study, the third-generation NDVI (NDVI3g) data were used, and they are the newest dataset derived from the Advanced Very High Resolution Radiometer (AVHRR) produced by the Global Inventory Monitoring and Modelling Studies (GIMMS) (Pinzon and Tucker, 2014). The dataset was summarized fortnightly at a spatial resolution of approximately 8 km for the period from 1982 to 2012, which had already been pre-processed to compensate for sensor degradation, data calibration, the effects of cloud cover and to remove the effects of stratospheric aerosols (Neigh *et al.*, 2008; Zeng *et al.*, 2013). To evaluate the changes in the NDVI appropriately, we used the Harmonic Analysis of NDVI Time-series (HANTS) to screen for and remove the outliers (Jong *et al.*, 2011; Roerink *et al.*, 2000). Then, the yearly maximum NDVI ($NDVI_{max}$) in the smoothed half-monthly time series was selected to evaluate the interannual variability in vegetation. The reasons for using the $NDVI_{max}$ are: (1) the $NDVI_{max}$ values are highly correlated with the average NDVI ($NDVI_{avg}$) during the growing season (April to October) (the R^2 value between $NDVI_{max}$ and $NDVI_{avg}$ from 1982–2011 is larger than 0.6 in nearly 80% of the basin; the R^2 value between the multi-year average $NDVI_{max}$ and $NDVI_{avg}$ in the entire basin is 0.52); and (2) in order to consider the delayed effects of meteorological factors on vegetation growth (this will be introduced later), the average period of the NDVI should be shorter than the delayed time, if possible. $NDVI_{max}$ is an instantaneous value, and thus it is appropriate for studying the delayed effects.

Air temperature and precipitation are two key climatic factors that are commonly used as explanatory variables of vegetation growth (Piao *et al.*, 2011). The daily precipitation data from 1982 to 2011 were obtained from a grid product with a spatial resolution of 0.25° and was provided by the National Meteorological Information Center (Shen *et al.*, 2010). The surface air temperature at a 2-m height was recorded from 21 stations around the basin (Figure 1(a)) and was provided by the China Meteorological Science Data Sharing Service System (http://cdc.cma.gov.cn/). As a supplement to the gridded precipitation, station-based precipitation data with a lower spatial resolution but longer time span (during 1960–2010) than the gridded precipitation were obtained from the same meteorological stations that recorded the air temperature. The station-based temperature and precipitation data were interpolated onto the NDVI grid using the Inverse Distance Weighting (IDW) interpolation method (Tomczak, 1998), with the aid of a digital elevation model (USGS/NASA Shuttle Radar Topography Mission (SRTM) system), which has a horizontal resolution of 90 m.

The streamflow data of the outlet of the basin were provided by the Hydrological Bureau of the Ministry of Water Resources of China. In addition, the latest version of Chinese high-resolution (100 m) land use type of 2010 was obtained from the Institute of Remote Sensing and Digital Earth, Chinese Academy of Sciences (Zhang *et al.*, 2014). The land use type in 1985 was provided by the Institute of Geographic Sciences of Natural Resources Research, Chinese Academy of Sciences (Liu *et al.*, 2003). The census data of the annual grazing size (the number of livestock) and crop yield of each county in the basin were obtained from the Inner Mongolian, Jilin and Liaoning Statistical Yearbooks.

Detection of the trends and changing points

The trends in the time series were detected using the linear regression model, which is expressed as follows:

$$y_i = \alpha x_i + \beta + \varepsilon \tag{1}$$

where $x_i(i = 1, 2 \cdots n)$ is the independent variable (time in this case) and $y_i(i = 1, 2 \cdots n)$ is the corresponding dependent variable (values of precipitation, temperature, or NDVI); α and β are the regression coefficients; and ε is the estimation error of the linear regression. The regression effects are considered significant at the significance level of 5% using the T-test.

The changing points (CP) in the time series of meteorological factors and NDVI were detected using a piecewise regression model (Toms and Lesperance, 2003; Sun *et al*., 2011):

$$y_i = \begin{cases} \alpha_1 x_i + \beta_1 + \varepsilon & i \le k \\ \alpha_1 x_i + \beta_1 + \alpha_2 (x_i - x_k) + \beta_2 + \varepsilon & i > k \end{cases} \tag{2}$$

where k is the timing of CP; α_1 and β_1 are the regression coefficient and intercept before CP, respectively; and $(\alpha_1 + \alpha_2)$ and $(\beta_1 + \beta_2 - \alpha_2 x_k)$ are the regression coefficient and intercept after CP, respectively. The regression coefficients and intercepts were estimated using the least squares method.

Attributing the trends in vegetation

The linear regression model is usually applied to the annual (or seasonal average) NDVI and annual (or seasonal average) meteorological factors (Wang *et al*., 2013; An *et al*., 2014) to identify the reasons for the vegetation trends and can be single or multiple (Peng *et al*., 2011; Liu *et al*., 2013). This type of model successfully demonstrates the responses of the temporal changes in the NDVI to climate changes; however, it ignores the nonlinear responses of the vegetation to climate variability (Wang *et al*., 2003; Liu *et al*., 2015) and fails to consider the delayed effects of climatic factors on the NDVI (Piao *et al*., 2006; Song and Ma, 2011), which are shown to have great impacts on the seasonal variation in the NDVI. We examined the relationships between the NDVI and the climatic factors (i.e. precipitation and temperature) in the forestland, which has relatively little human interference (Figure 3), and found that precipitation has a significant nonlinear relationship with $NDVI_{max}$, showing that precipitation is no longer a limiting factor of $NDVI_{max}$ when it is larger than a certain threshold. Air temperature has a negative effect on $NDVI_{max}$, which was consistent with the long-term field study in Inner Mongolia (Bai *et al*., 2004; Guo *et al*., 2006).

Therefore, by incorporating the nonlinear relationship between $NDVI_{max}$ and precipitation and the linear relationship between $NDVI_{max}$ and temperature, a binary nonlinear regression model, which is modified from the work of Liu *et al*. (2013) and considers the delayed effects, was employed in this study to simulate $NDVI_{max}$ in the natural status:

$$NDVI_{\max} = \frac{\alpha}{1 + \exp[\beta(Pi - \gamma)]} + \delta Tj + \phi \tag{3}$$

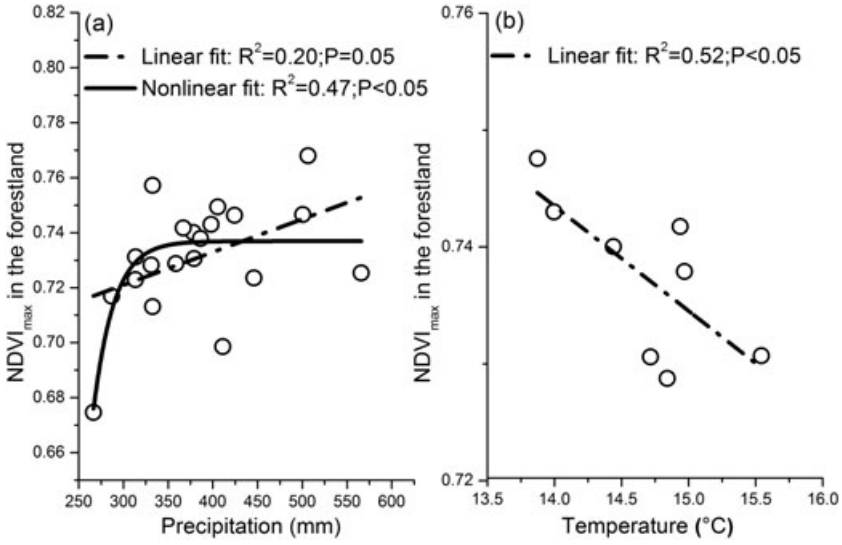

Figure 3. Curve fit between (a) precipitation and $NDVI_{max}$ and (b) temperature and $NDVI_{max}$ in forestland. The temperature and $NDVI_{max}$ data were selected under similar precipitation conditions, when the annual precipitation was between 355 and 400 mm (this range contains the most data points); the precipitation and $NDVI_{max}$ data were selected under similar temperature conditions, when the annual mean temperature was between 13.9 and 15.2 °C.

where α, β, γ, δ and ϕ are regression coefficients. P and T are the cumulative precipitation and average temperature, respectively; i and j are varying periods before the time when the maximum NDVI appears, for which the specified periods for precipitation and temperature can be different.

For a better understanding of the model, we present an example here. By assuming that the $NDVI_{max}$ appears in August, the periods i and j can be selected from the matrix composed of the combination of the periods listed in Table I. The leading month and length of months are the first month and the number of months, respectively. The time range in the table is the period when the meteorological factors may have an effect on $NDVI_{max}$ (the number '1' is for January and '8' is for August). For example, the leading month of '1' and a length of months of 1 will result in January (1), while the leading month of '2' and the length of months of 3 will result in the period from February to April (2–4). As a result, there are 36 values in total, the different specified periods for precipitation and temperature leading to 1296 combinations. The combination that results in the highest value for the coefficient of determination (R^2) of the multiple nonlinear regressions is accepted. Because the plant types are annual grass, shrub, crop and broadleaf deciduous tree, we assumed that the climate conditions in the previous year had no impacts on the vegetation growth in the current year. By applying the model, we found that the months that exhibit the most effects because of the climatic factors are May, June and July in this basin.

Using Equation 3, the estimated $NDVI_{max}$ was identified as the 'climate-induced $NDVI_{max}$' (Liu *et al*., 2013). The difference between the observed and estimated $NDVI_{max}$ is assumed to result from the effects of anthropogenic factors. The degree to which the estimated $NDVI_{max}$ variations could explain the observed $NDVI_{max}$ variations can be considered as the impact of climate change on the vegetation variations. Therefore, the ratio (denoted as K) of the trend in the estimated $NDVI_{max}$ to the trend in the observed $NDVI_{max}$ can serve as the degree to which the observed $NDVI_{max}$ is affected by climate variability. When K is larger than 0.5, we determined that the vegetation trend was dominated by climate variability; otherwise, it was dominated by anthropogenic factors.

Table I. Period matrix for the binary nonlinear regression model.

Length of months / Leading month	1	2	3	4	5	6	7	8
1	1	1-2	1-3	1-4	1-5	1-6	1-7	1-8
2	2	2-3	2-4	2-5	2-6	2-7	2-8	
3	3	3-4	3-5	3-6	3-7	3-8		
4	4	4-5	4-6	4-7	4-8			
5	5	5-6	5-7	5-8				
6	6	6-7	6-8					
7	7	7-8						
8	8							

RESULTS AND DISCUSSION

Evaluation of the regression model

Ideally, a rigorous evaluation of this model is impossible because of the influences of human activities on the NDVI and the different parameters in Equation 3 for different pixels. Therefore, we assumed that forestland has relatively little human interference, and that the neighbouring pixels have similar parameters in Equation 3. First, we compared our model and the model proposed by Liu *et al*. (2013) using two randomly selected pixels in the forest (the surrounding eight pixels are also forest) (the selected pixels were marked in Figure 1(a)) to show how our model was improved by incorporating the nonlinear relationship between the $NDVI_{max}$ and precipitation. Figure 4 shows the time series of the $NDVI_{max}$ in the two pixels. The interannual variability of $NDVI_{max}$ can well be explained using Equation 3. For these two pixels, the nonlinear model is better (i.e. higher R^2 and lower RMSE) than the linear model used in Liu *et al*. (2013). In particular, the nonlinear model predicted the $NDVI_{max}$ much better in extremely dry years, such as 2000 and 2009.

To further evaluate the regression model, we selected a group of adjacent forestland pixels and divided them into two sub-groups for a 'quasi-cross-validation'. We employed precipitation and temperature, as well as the $NDVI_{max}$ data from one group to calibrate parameters in Equation 3 and those from another group to validate the model. The statistical indexes in both the calibration and validation periods ($R^2 = 0.68$, $P < 0.05$ and $R^2 = 0.58$, $P < 0.05$, respectively) indicated that the model was competent for simulating the vegetation changes in response to the climatic factors (Rohlf and Sokal, 1969).

However, we should acknowledge that this method has potential uncertainties because of the choices of climatic variables, data quality and model assumptions. Potential errors may be introduced when the differences between the estimated $NDVI_{max}$ and observed $NDVI_{max}$ are used to infer the relative contribution of the anthropogenic factors. In addition to the regression method used in our study, process-based ecosystem models (Sitch *et al*., 2008; Piao *et al*., 2013) can also be used to attribute the trends of vegetation. However, process-based ecosystem models have two main sources of uncertainties. First, large uncertainties may arise from the complex model structure and large number of parameters (Piao *et al*., 2013). Second, these models cannot usually simulate the effects of human activities, such as agricultural management and grazing (Piao *et al*., 2015), which results in large uncertainties in

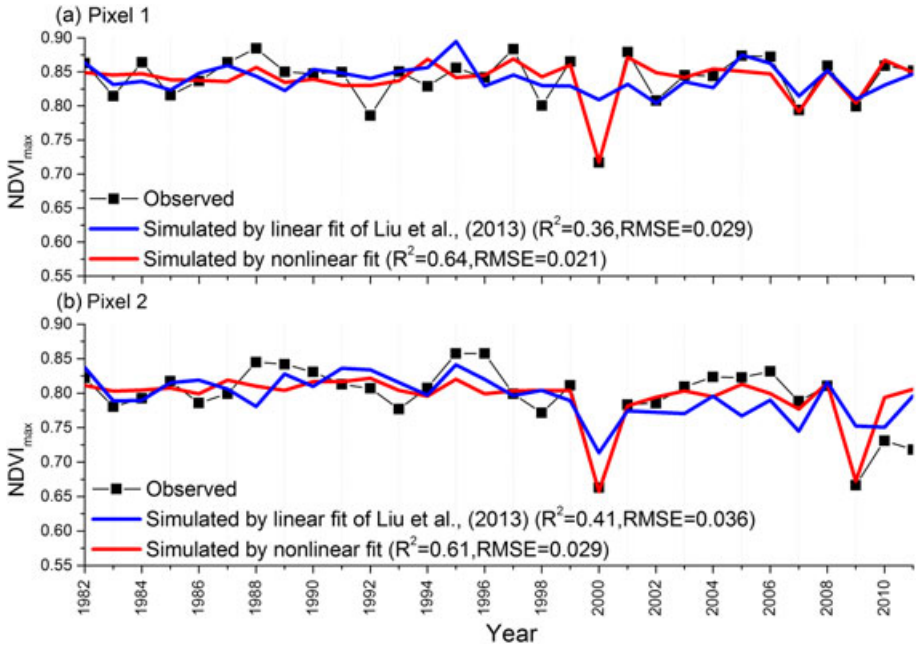

Figure 4. Interannual variations in the simulated and satellite observed $NDVI_{max}$ of two pixels (marked in Figure 1) within the forestland.

the model-estimated trends of the leaf area index. Our recent study also demonstrated that there were large uncertainties when simulating the leaf area index in a typical process-based ecosystem model (Lei *et al*., 2014). Therefore, there is still no precise method that can accurately simulate the variations in vegetation growth; additional mechanisms of vegetation growth should be investigated in ecohydrological studies.

Spatial patterns of the trends in $NDVI_{max}$, precipitation and temperature

The growing season is comprised of the entire time of active vegetation, including the green-up, maturity and senescence periods (Guan *et al*., 2014). Hence, we focused on the climate changes during the growing season, which generally occurs from April to October in this region. We calculated the cumulative precipitation and average temperature from April to October in each year from 1982 to 2011 (Figure 5).

Figure 5(a) and (d) display the spatial patterns of the complete and significant trends of $NDVI_{max}$ in the basin over the past three decades, respectively. The spatial pattern of the trends in $NDVI_{max}$ shows a significant difference between the north and the south. Approximately 41.5% of the entire basin showed negative trends in vegetation, mainly in the north (10% of the basin experienced a significant decrease in the vegetation rate of $-0.0024\,year^{-1}$). Meanwhile, 58.5% of the watershed experienced positive trends, primarily in the south (29% of the basin experienced a significant increase in the vegetation rate of $0.0031\,year^{-1}$). Figure 5(b) and (e) illustrate the spatial distribution of the negative and significant trends in precipitation throughout the basin, indicating drying of the entire watershed, particularly in the north. Figure 5(c) and (f) show significant positive trends in temperature throughout the basin, which indicates that the entire watershed was warming. The positive trends in the southern temperature were even more significant than those in the northern temperature.

Temporal variations in $NDVI_{max}$, precipitation and temperature

Figure 6 illustrates the temporal variations in the $NDVI_{max}$, precipitation and temperature averaged over the entire basin. The results show that $NDVI_{max}$ exhibited an insignificant increasing trend over the entire study period (Slope = $0.0006\,year^{-1}$, $R^2 = 0.05$, $P > 0.05$) and an insignificant drop in 2000. However, $NDVI_{max}$ exhibited a significant increasing trend before 2000 (Slope = $0.0035\,year^{-1}$, $R^2 = 0.64$, $P < 0.05$), which is consistent with the findings of Piao *et al*. (2005), who revealed an overall reversion of desertification in arid and semiarid regions in China from 1982 to 1999. The precipitation exhibited a significant decreasing trend (Slope = $-3.7\,mm\,year^{-1}$, $R^2 = 0.18$, $P < 0.05$), as well as a significant drop in 1999. The statistical results show that the mean annual precipitation before 1999 was higher than the mean annual value from 1982 to 2011, and the mean annual precipitation after 1999 was 14.5% lower than the mean annual value from 1982 to 2011. Therefore, the long-

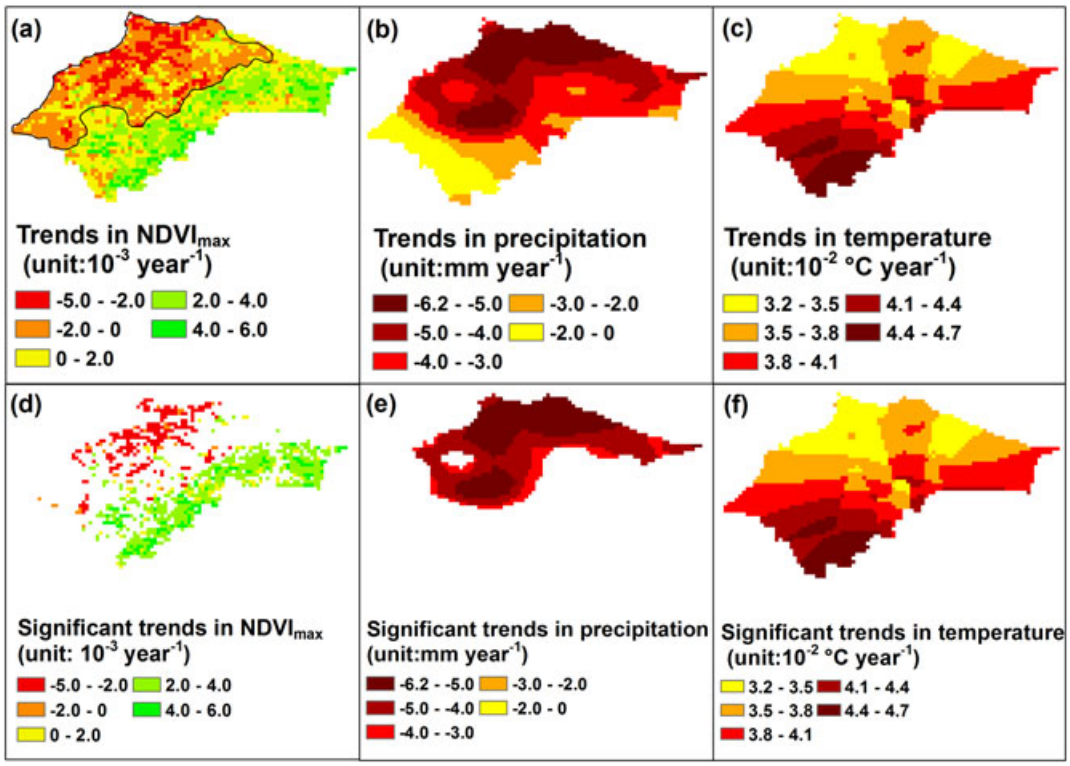

Figure 5. (a–c) Spatial distributions of the trends in the $NDVI_{max}$, cumulative precipitation and mean temperature from April to October and (d–f) significant trends in the $NDVI_{max}$, cumulative precipitation and mean temperature at a significance level of 0.05. The black coiled line in Figure 5(a) is the boundary of the northern part with decreasing $NDVI_{max}$ and, accordingly, the southern part with increasing $NDVI_{max}$ comprises the rest of the basin.

term decreasing trend in precipitation was not because of a gradual change, but instead to a multiyear reduction in precipitation from 1999 to 2011. This phenomenon suggested that the degradation in vegetation may be because of short-term drought, but not a long-term climate change, as reported by Li *et al.* (2014), who showed that the Horqin sand was not a desertification region in the mid-Holocene (approximately 6000 years ago) because more moisture was present during that time than at the present day. In particular, we observed that the precipitation decreased considerably in 1999, but the $NDVI_{max}$ reached its highest value in the same year (Figure 6(a–b)). We found that the significant decrease in precipitation in 1999 was mainly because of the significant decrease in precipitation in August, when the monthly precipitation was the third highest in that year. Meanwhile, in most regions, the NDVI reached its maximum in August. Recall that the most effective months for vegetation growth are May, June and July; we speculate that the decrease in precipitation in August had no direct effect on the $NDVI_{max}$ in this year. The air temperature exhibited a significant increasing trend ($\text{Slope} = 0.038\ ^{\circ}\text{C year}^{-1}$, $R^2 = 0.34$, $P < 0.05$) and a significant change point in 1998. The gradual trends in temperature in the two sub-periods were not significant. After 1998, an insignificant decreasing trend is revealed, which indicates that the climate warming may have slowed down in recent years. Similarly, other researchers also reported that climate warming slowed down in the mid-1990s in other areas of China (Liu and Lei, 2015).

Based on the spatial pattern of trends in $NDVI_{max}$ (Figure 5(a)), we divided the basin into a northern part with decreasing $NDVI_{max}$ and a southern part with increasing $NDVI_{max}$ to remove the offset effect in the areal average. The northern and southern areas accounted for 41.5% and 58.5% of the total area, respectively. According to the land use map of 2010, the northern part is dominated by natural vegetation, with grasslands and forestlands occupying more than 68% and cropland only accounting for 9%. In the southern part, the dominant land use types are croplands and grasslands, which occupy 47% and 30%, respectively.

Figure 7 illustrates that the $NDVI_{max}$ in the northern part exhibited a significant decreasing trend ($\text{Slope} = -0.0015\ \text{year}^{-1}$, $R^2 = 0.20$, $P < 0.05$) and a significant change point in 2000, with an insignificant increasing trend prior to 2000 ($\text{Slope} = 0.0007\ \text{year}^{-1}$, $R^2 = 0.04$, $P > 0.05$) and an insignificant decreasing trend after 2000 ($\text{Slope} = -0.0009\ \text{year}^{-1}$, $R^2 = 0.01$, $P > 0.05$). In the southern part, the $NDVI_{max}$ exhibited a significant increasing trend ($\text{Slope} = 0.002\ \text{year}^{-1}$, $R^2 = 0.37$, $P < 0.05$), and an insignificant change-point with signifi-

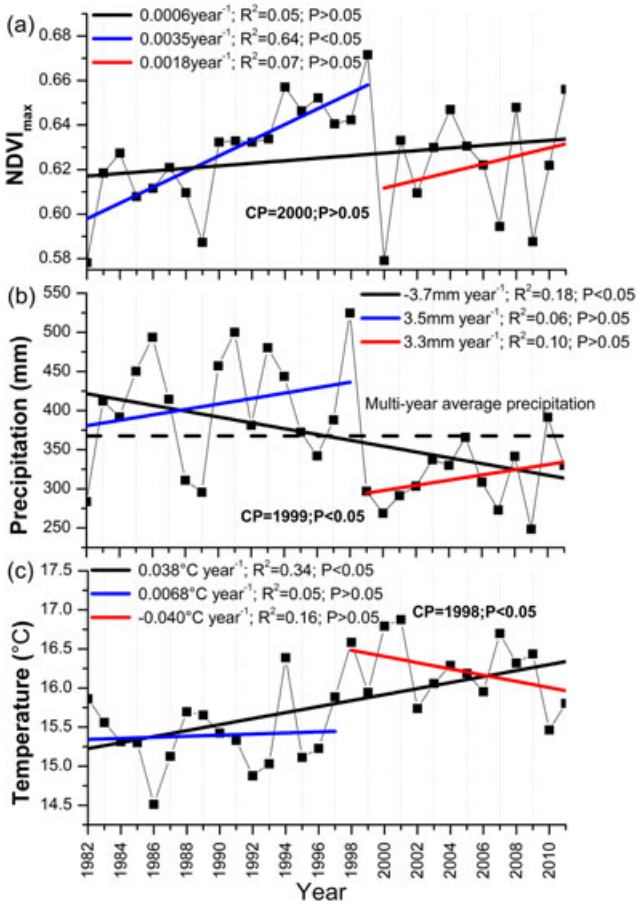

Figure 6. Interannual variations in the basin-averaged (a) $NDVI_{max}$, (b) cumulative precipitation and (c) mean temperature during April–October. Changing points (CP) of the trends estimated by least-squares linear regression are shown. The black lines indicate the linear fits during the period from 1982 to 2011, the blue lines indicate the linear fits before the CP of the corresponding trend and the red lines indicate the linear fits after the CP of the corresponding trend.

cant increasing trends occurred prior to 2000 (Slope = 0.005 year^{-1}, $R^2 = 0.81$, $P < 0.05$) and after 2000 (Slope = 0.004 year^{-1}, $R^2 = 0.36$, $P < 0.05$). The trends in $NDVI_{max}$ in the southern part from 1982 to 2000 are seven times larger than those in the northern part. The precipitation decreased in both the northern and southern parts ($R^2 = 0.22$, $P < 0.05$; $R^2 = 0.14$, $P < 0.05$, respectively), but the decreasing trend in the northern part was larger than that in the south. Moreover, there was a significant decrease in precipitation in both regions in 1999. The temperature in both the northern and southern parts exhibited significant increasing trends ($R^2 = 0.30$, $P < 0.05$ and $R^2 = 0.34$, $P < 0.05$, respectively) and a significant increase in 1998. The temperature trends in both parts did not show significant changes before or after 1998. In summary, precipitation and temperature have similar temporal patterns in both parts, while there was a large difference in $NDVI_{max}$ between the north and south, which implies that other mechanisms may determine the vegetation trends.

Attribution and possible reasons for the vegetation trends

Based on the results of K, the ratio of the trend in vegetation estimated using Equation 3 to the observed trend in vegetation and the spatial distribution of the dominant factors of the vegetation changes in the entire basin are shown in Figure 8. Interestingly, there were distinguishing differences in the causes of the vegetation trends between the north and south, although the climatic factors varied similarly in the two parts. The area in which the change in $NDVI_{max}$ is dominated by the climatic factors occupies 53.6% of the entire basin, while the remainder can be considered to be dominated by non-climatic factors. In the northern part, approximately 82.7% of the $NDVI_{max}$ reductions can be attributed to climate variability, whereas 67.0% of the $NDVI_{max}$ increases in the southern part can be explained by anthropogenic activities (Figure 8).

According to Figure 9, we also found that the $NDVI_{max}$ variability was well interpreted by the precipitation variability in the non-cropland, which was mainly distributed in the north, while $NDVI_{max}$ was not relevant

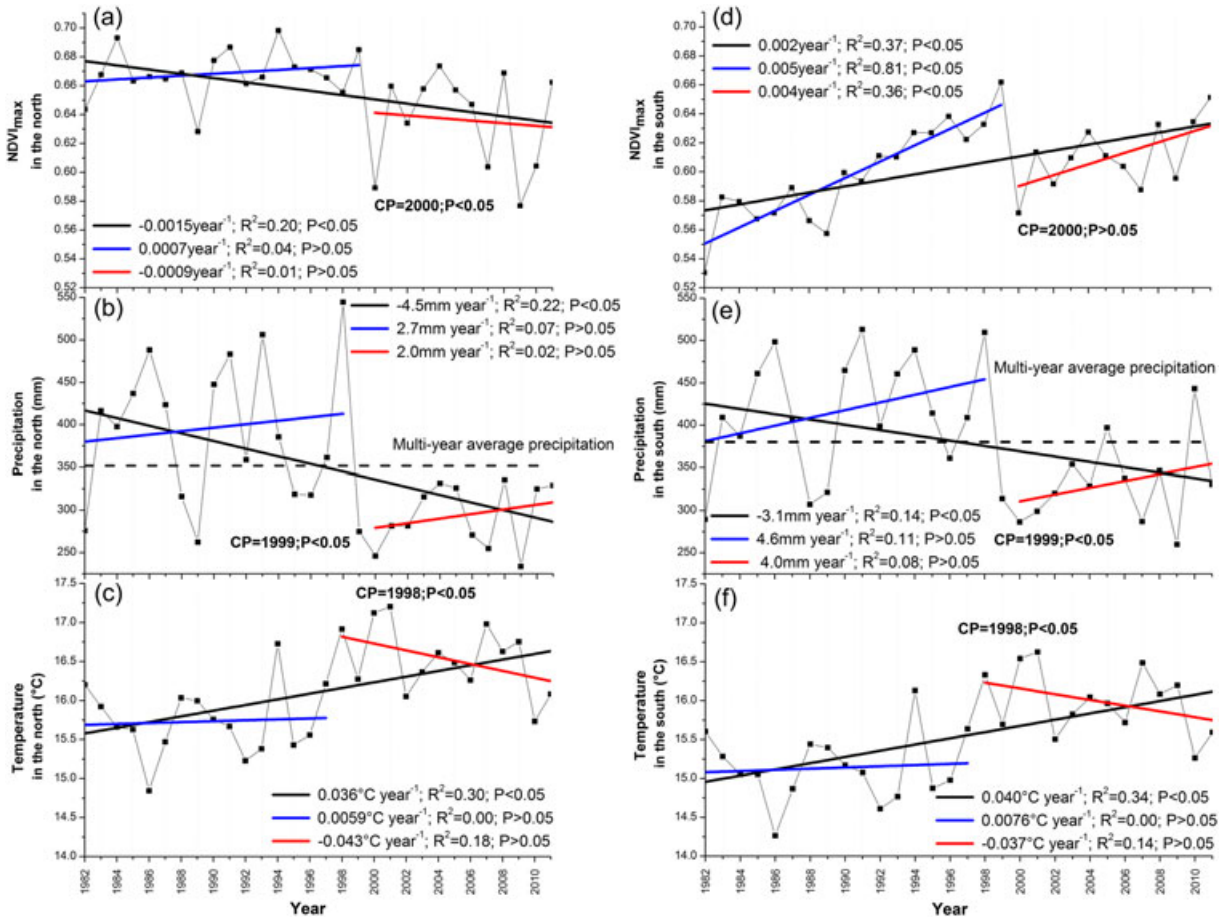

Figure 7. The data are the same as Figure 6, but (a–c) are in the northern part (the corresponding boundary is plotted in Figure 5(a)) and (d–f) are in southern part.

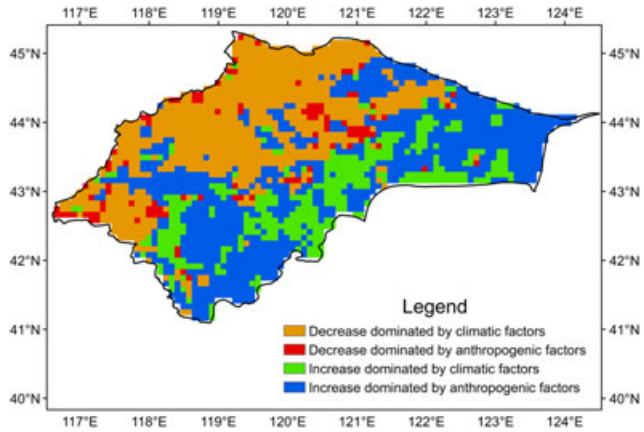

Figure 8. Distribution of the dominant factors controlling the vegetation trends in the Xiliao River Basin.

to the precipitation in the cropland, which was mainly distributed in the south. The multiyear reductions in precipitation after 1999 may have made a significant contribution to the decrease in $NDVI_{max}$ in the northern part, which was supported by a study using a physiological ecosystem model (Yuan *et al.*, 2014). On the other hand, although the warming was more significant in the south than in the north, the promoting effect of increasing temperature was weaker than the effect of cropland management.

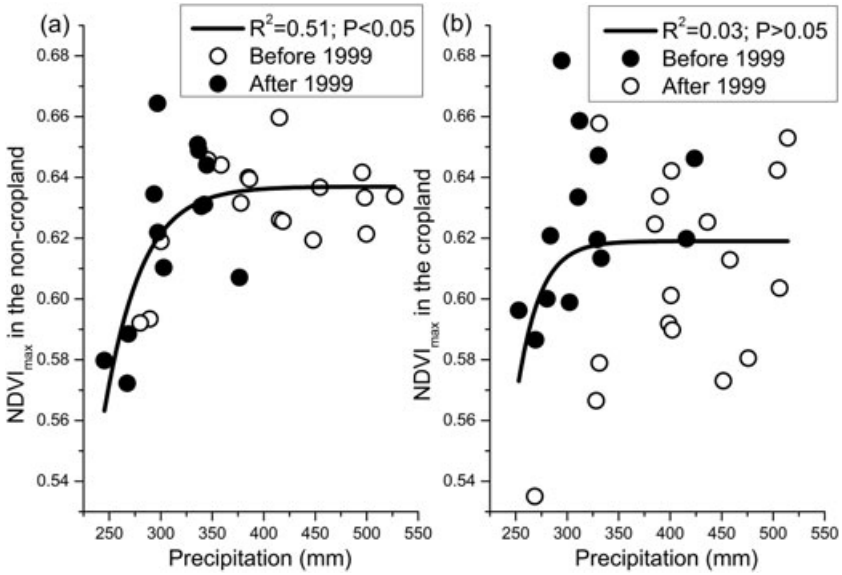

Figure 9. Relationships between $NDVI_{max}$ and precipitation in (a) non-cropland and (b) cropland.

To further explore the effects of human activities on the changes in vegetation, we calculated the significant trends ($p < 0.05$) in the NDVI residuals by subtracting the estimated $NDVI_{max}$ from the observed $NDVI_{max}$. Positive (negative) trends in the NDVI residuals indicate that human activities promote (hinder) vegetation growth. Using positive trends as an example, positive trends in both the NDVI and NDVI residuals imply a more intense influence

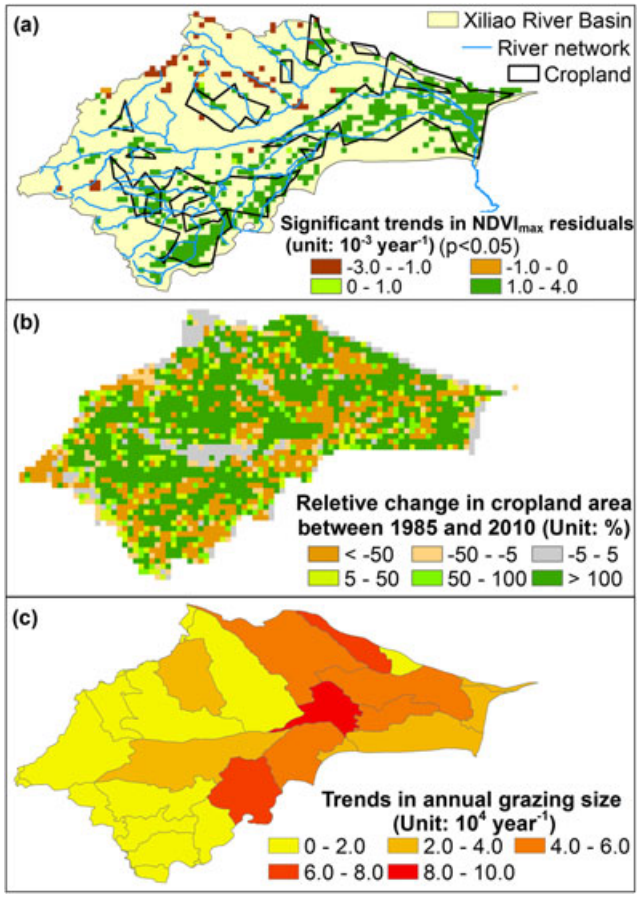

Figure 10. Spatial distributions of (a) the trends in the $NDVI_{max}$ residuals, (b) the relative changes in cropland area and (c) the trends in grazing size.

of positive human activities, while positive trends in the NDVI and negative trends in the NDVI residuals indicates less disturbances by negative human activities.

Figure 10(a) showed that the distribution of the significant trend in the NDVI residuals is mainly positive and generally consistent with the distribution of cropland, which implies that vegetation greening in the southern part may be mainly because of the intensifying cropland management. In general, the water-related cropland management to promote crop growth includes increasing the amount of irrigation and/or an expanding the area being irrigated. To distinguish these two types of cropland management, we calculated the changes in the cropland area in each grid between 1985 and 2010 (Figure 10(b)). The results demonstrate the cropland area increased by a total of 16%, which is consistent with the conclusions from previous studies, which also reported that the Horqin Sandy land had doubled the cropland area over the past three decades (Bagan *et al*., 2010). However, the spatial pattern of changes in the cropland area was not generally consistent with the trends in the NDVI residuals. We further analysed the interannual variations in the annual discharge of the outlet of the basin (see Figure 1(b)), showing that the main stream dried up in the 1970s and 2000s (Figure 11). Although the interannual variability of precipitation was high, the dry-up demonstrated, at a minimum, that a large amount of water use began in the 1960s. This large water withdrawal was because of the establishment of several reservoirs (the total storage capacity of these reservoirs was $3.32 \times 10^9\,m^3$ (Wang and Li, 2007)) in 1958 in three major streams (Figure 1(b)). Of these, the Hongshan reservoir, lying at the basin outlet, is the largest reservoir in northeast China, with a storage capacity of $2.56 \times 10^9\,m^3$, and controls the majority of cropland irrigation in the Xiliao River basin. During our study period (1982–2011), the annual runoff decreased significantly from 4.0 mm in 1980s to 0.3 mm in 2000s, implying that much more water was used for irrigation. The statistics also showed that both an increasing amount of irrigation and an expansion of the irrigated area were observed in the two largest cities (Tongliao and Chifeng) in the basin (Wang and Li, 2007). A modelling study in the upper reach of the Xiliao River basin also identified that human activities (a significant increase in the irrigated area) were the main driving factors for the streamflow reduction, with contributions of approximately 90% (Yong *et al*., 2013). Therefore, the significant vegetation greening in cropland may be because of both an increasing amount of irrigation and/or an expansion of the irrigated area. The phenomenon of vegetation greening in cropland was also indirectly demonstrated by the significant increase in crop yield over the entire basin (2.7×10^5 ton year^{-1}, $p < 0.01$, during 1992–2011). Our findings were different from the reports of many other researchers, who showed that vegetation greening is primarily determined by climate warming (Bogaert *et al*., 2002; Jia *et al*., 2009; Dai *et al*.,

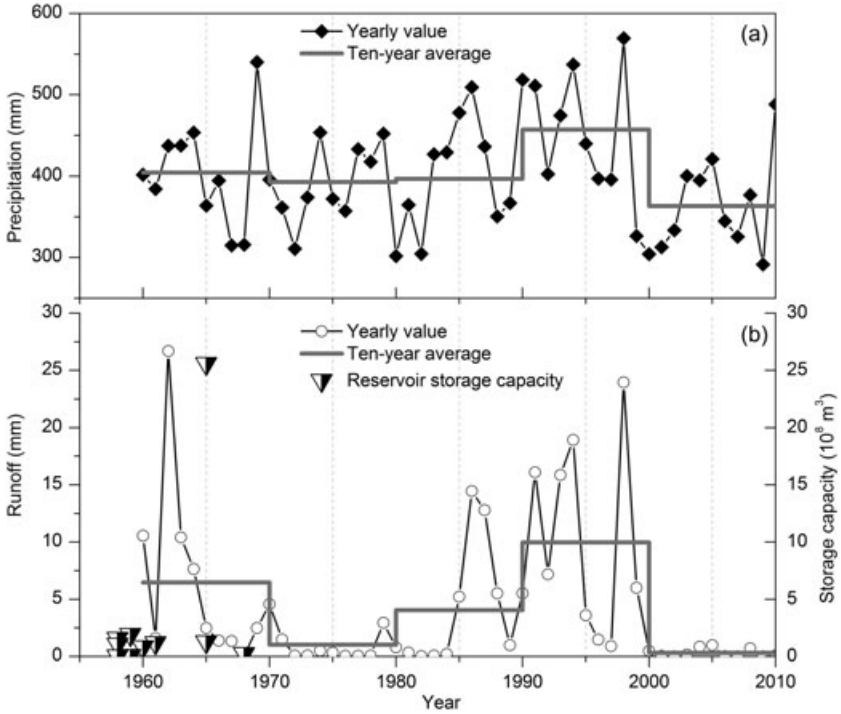

Figure 11. Long-term variations in (a) the basin-averaged annual precipitation and (b) annual streamflow of the basin outlet. The times at which the reservoirs were established and their respective storage capacities are shown. The positions of the outlets and reservoirs are drawn in Figure 1(b).

2014) and was consistent with a study showing that the pronounced increase in the NDVI of cropland almost certainly stemmed from changes in the primary crop type and the advances in agricultural management in Inner Mongolia (Guo *et al*., 2014).

The dominant roles of climatic factors in vegetation degradation in the northern part can also be indirectly supported by the mismatch between the distributions of the trends in the NDVI and grazing size (Figure 10(c)). Theoretically, the magnitude of the decreasing trend in vegetation should be generally consistent with that of the increasing trend in grazing size, if the effects of grazing on vegetation are large. In fact, although grazing size increased throughout the basin ($5.8 \times 10^5\,\mathrm{year}^{-1}$, $p < 0.01$, during 1992–2011), its spatial pattern cannot explain the spatial distribution of NDVI browning. This finding was remarkably different from a previous study showing that degradation in the Mongolian Steppe was closely related to the spatial variations in goat density (Liu *et al*., 2013).

CONCLUSIONS

The climate of the Xiliao River basin in northeast China has been becoming warmer and dryer over the past three decades. However, the vegetation trends in the north and south of the basin were obviously different: vegetation is mainly browning in the north, which is largely occupied by natural vegetation, and is mainly greening in the south, which is largely occupied by cropland. Using an empirical model, we found that 82.7% of the vegetation degradation in the north could be attributed to climate variability, rather than the increasing grazing size. Specifically, the multiyear reductions in precipitation from 1999 to 2011 were mainly responsible for the vegetation degradation, despite the rising air temperature. In the southern part, 67.0% of the vegetation greening could be explained by cropland management, rather than the significantly increasing temperature.

In terms of desertification control, our findings reveal that the natural ecosystem in the north is already quite fragile, because of the changing environment, and thus grazing size should be strictly limited in the future. The greening in cropland appears to be beneficial for desertification control. However, it is based on the large amount of water withdrawals from rivers. This overexploitation of water resources has already caused serious environmental problems, such as river dry-up in relatively dry years, and imposes challenges to the sustainable development of ecosystems. Therefore, it will also be an urgent task of controlling agricultural development for protecting the environment in this semi-arid desertified watershed.

ACKNOWLEDGEMENTS

This research was supported by the National Natural Science Foundation of China (Project Nos. 51139002), the Basic Research Fund Program of State Key Laboratory of Hydroscience and Engineering (Grant No. 2014-KY-04) and the Ministry of Education Innovation Team Development Program (IRT13069). The authors would like to thank Dr. A.W. Jayawardena from the University of Hong Kong for improving the manuscript.

REFERENCE

An Y, Gao W, Gao Z. 2014. Characterizing land condition variability in Northern China from 1982 to 2011. *Environmental Earth Sciences* **72**: 663–676. DOI:10.1007/s12665-013-2987-6.

Bagan H, Takeuchi W, Kinoshita T, Bao Y, Yamagata Y. 2010. Land cover classification and change analysis in the Horqin Sandy Land from 1975 to 2007. *IEEE Journal of Selected Topics in Applied Earth Observations and Remote Sensing* **3**: 168–177. DOI:10.1109/JSTARS.2010.2046627.

Bai YF, Han XG, Wu JG, Chen ZZ, Li LH. 2004. Ecosystem stability and compensatory effects in the Inner Mongolia grassland. *Nature* **431**: 181–184.

Bao G, Qin Z, Bao Y, Zhou Y, Li W, Sanjjav A. 2014. NDVI-based long-term vegetation dynamics and its response to climatic change in the Mongolian Plateau. *Remote Sensing* **6**: 8337–8358. DOI:10.3390/rs6098337.

Bogaert J, Zhou L, Tucker CJ, Myneni RB, Ceulemans R. 2002. Evidence for a persistent and extensive greening trend in Eurasia inferred from satellite vegetation index data. *Journal of Geophysical Research* **107**ACL-4: . DOI:10.1029/2001JD001075.

Dai L, Zhang L, Wang K, Wang R. 2014. Response of vegetation to climate change in the drylands of East Asia. *IOP Conference Series: Earth and Environmental Science* **17**: 2081. DOI:10.1088/1755-1315/17/1/012081.

Goetz SJ, Bunn AG, Fiske GJ, Houghton R. 2005. Satellite-observed photosynthetic trends across boreal North America associated with climate and fire disturbance. *Proceedings of the National Academy of Sciences of the United States of America* **102**: 13521–13525. DOI:10.1073/pnas.0506179102.

Guan K, Wood EF, Medvigy D, Kimball J, Pan M, Caylor KK, Sheffield J, Xu X, Jones MO. 2014. Terrestrial hydrological controls on land surface phenology of African savannas and woodlands. *Journal of Geophysical Research, Biogeosciences* **119**: 1652–1669. DOI:10.1002/2013JG002572.

Guo R, Wang XK, Ouyang ZY, Li YN. 2006. Spatial and temporal relationships between precipitation and ANPP of four types of grasslands in northern China. *Journal of Environmental Sciences* **18**: 1024–1030.

Guo L, Wu S, Zhao D, Yin Y, Leng G, Zhang Q. 2014. NDVI-based vegetation change in Inner Mongolia from 1982 to 2006 and its relationship to climate at the biome scale. *Advances in Meteorology* **2014**692068: . DOI:10.1155/2014/692068.

Han C, Chen R, Liu J, Yang Y, Qing W. 2010. A discuss of the separating solid and liquid precipitations. *Journal of Glaciology Geocryology* **32** (2): 249–256(in Chinese with English abstract).

Hilker T, Natsagdorj E, Waring RH, Lyapustin A, Wang Y. 2014. Satellite observed widespread decline in Mongolian grasslands largely due to overgrazing. *Global Change Biology* **20**: 418–428. DOI:10.1111/gcb.12365.

Jia GJ, Epstein HE, Walker DA. 2009. Vegetation greening in the Canadian Arctic related to decadal warming. *Journal of Environmental Monitoring* **11**: 2231–2238. DOI:10.1039/b911677j.

Jong RD, Bruin SD, Wit AD, Schaepman ME, Dent DL. 2011. Analysis of monotonic greening and browning trends from global NDVI time-series. *Remote Sensing of Environment* **115**: 692–702. DOI:10.1016/j.rse.2010.10.011.

Kawabata A, Ichii K, Yamaguchi Y. 2001. Global monitoring of interannual changes in vegetation activities using NDVI and its

relationships to temperature and precipitation. *International Journal of Remote Sensing* **22**: 1377–1382. DOI:10.1080/01431160119381.

Lei H, Yang D, M H. 2014. Impacts of climate change and vegetation dynamics on runoff in the mountainous region of the Haihe River basin in the past five decades. *Journal of Hydrology* **511**: 786–799.

Li Q, Wu H, Guo Z, Yu Y, Ge J, Wu J, Zhao D, Sun A. 2014. Distribution and vegetation reconstruction of the deserts of northern China during the mid-Holocene. *Geophysical Research Letters* **41**: 5184–5191. DOI:10.1002/2014GL059952.

Liu X, Zhu X, Li S, Liu Y, Pan Y. 2015. Changes in growing season vegetation and their associated driving forces in China during 2001–2012. *Remote sensing* **7**: 15517–15517. DOI:10.3390/rs71115517.

Liu Y, Lei H. 2015. Responses of natural vegetation dynamics to climate drivers in China from 1982 to 2011. *Remote Sensing* **7**: 10243–10268. DOI:10.3390/rs70810243.

Liu J, Liu M, Zhuang D, Zhang Z, Deng X. 2003. Study on spatial pattern of land-use change in China during 1995–2000. *Science in China Series D: Earth Sciences* **46**: 373–384.

Liu YY, Evants JP, McCabe MF. 2013. Changing climate and overgrazing are decimating Mongolian steppes. *PLoS ONE* **8**e57599: . DOI:10.1371/journal.pone.0057599.g001.

Mu SJ, Chen YZ, Li JL, Ju WM, Odeh IOA, Zou XL. 2013. Grassland dynamics in response to climate change and human activities in Inner Mongolia, China between 1985 and 2009. *The Rangeland Journal* **35**: 315–329. DOI:10.1071/RJ12042.

Myneni RB, Hall FG, Sellers PJ, Marshak AL. 1995. The interpretation of spectral vegetation indexes. *IEEE Transactions on Geoscience and Remote Sensing* **33**: 481–486.

Neigh CS, Tucker CJ, Townshend JR. 2008. North American vegetation dynamics observed with multi-resolution satellite data. *Remote Sensing of Environment* **112**: 1749–1772. DOI:10.1016/j.rse.2007.08.018.

Peng S, Chen A, Xu L, Cao C, Fang J, Myneni RB, Pinzon JE, Tucker CJ, Piao S. 2011. Recent change of vegetation growth trend in China. *Environmental Research Letters* **6**: 044027. DOI:10.1088/1748-9326/6/4/044027.

Piao S, Fang J, Liu H, Zhu B. 2005. NDVI-indicated decline in desertification in China in the past two decades. *Geophysical Research Letters* **32**L06402: . DOI:10.1029/2004GL021764.

Piao S, Mohammat A, Fang J, Cai Q, Feng J. 2006. NDVI-based increase in growth of temperate grasslands and its responses to climate changes in China. *Global Environmental Change* **16**: 340–348. DOI:10.1016/j.gloenvcha.2006.02.002.

Piao S, Wang X, Ciais P, Zhu B, Wang T, Liu J. 2011. Changes in satellite-derived vegetation growth trend in temperate and boreal Eurasia from 1982 to 2006. *Global Change Biology* **17**: 3228–3239. DOI:10.1111/j.1365-2486.2011.02419.x.

Piao S, Sitch S, Ciais P, Sitch S, Ciais P, Friedlingstein P, Peylin P, Wang X, Ahlström A, Anav A, Canadell JG, Cong N, Huntingford C, Jung M, Levis S, Levy PE, Li J, Lin X, Lomas MR, Lu M, Luo Y, Ma Y, Myneni RB, Poulter B, Sun Z, Wang T, Viovy N, Zaehle S, Zeng N. 2013. Evaluation of terrestrial carbon cycle models for their response to climate variability and to CO_2 trends. *Global Change Biology* **19**: 2117–2132.

Piao S, Yin G, Tan J, Cheng L, Huang M, Li Y, Liu R, Mao J, Myneni RB, Peng S, Poulter B, Shi X, Xiao Z, Zeng N, Zeng Z, Wang Y. 2015. Detection and attribution of vegetation greening trend in China over the last 30 years. *Global Change Biology* . DOI:10.1111/gcb.12795.

Pinzon JE, Tucker CJ. 2014. A non-stationary 1981–2012 AVHRR NDVI3g time series. *Remote Sensing* **6**: 6929–6960. DOI:10.3390/rs6086929.

Reynolds JF, Smith DS, Lambin EF, Turner B, Mortimore M, Batterbury SP, Downing TE, Dowlatabadi H, Fernández RJ, Herrick JE, Sannwald EH, Jiang H, Leemans R, Lynam T, Maestre FT, Ayarza M, Walker B. 2007. Global desertification: Building a science for dryland development. *Science* **316**: 847–851. DOI:10.1126/science.1131634.

Roerink GJ, Menenti M, Verhoef W. 2000. Reconstructing cloudfree NDVI composites using Fourier analysis of time series. *International Journal of Remote Sensing* **21**: 1911–1917. DOI:10.1080/014311600209814.

Rohlf FJ, Sokal RR. 1969. *Statistical Tables*. W. H. Freeman and Company: San Francisco.

Runnström MC. 2000. Is northern China winning the battle against desertification? Satellite remote sensing as a tool to study biomass trends on the Ordos Plateau in semiarid China. *AMBIO: A Journal of the Human Environment* **29**: 468–476. DOI:10.1579/0044-7447-29.8.468.

D02114Shen Y, Xiong A, Wang Y, Xie P. 2010. Performance of high-resolution satellite precipitation products over China. *Journal of Geophysical Research* **115**: . DOI:10.1029/2009JD012097.

Sheng GL, Harazono Y, Oikawa T, Zhao HL, He ZY, Chang XL. 2000. Grassland desertification by grazing and the resulting micrometeorological changes in Inner Mongolia. *Agricultural and Forest Meteorology* **102**: 125–137. DOI:10.1016/S0168-1923(00)00101-5.

Sitch S, Huntingford C, Gedney N, Levy PE, Lomas M, Piao S, Betts R, Ciais P, Cox P, Friedlingstein P, Jones CD, Prentice IC, Woodward FI. 2008. Evaluation of the terrestrial carbon cycle, future plant geography and climate–carbon cycle feedbacks using five Dynamic Global Vegetation Models (DGVMs). *Global Change Biology* **14**: 2015–2039.

Song Y, Ma M. 2011. A statistical analysis of the relationship between climatic factors and the Normalized Difference Vegetation Index in China. *International Journal of Remote Sensing* **32**: 3947–3965. DOI:10.1080/01431161003801336.

Sun J, Wang X, Chen A, Ma Y, Cui M, Piao S. 2011. NDVI indicated characteristics of vegetation cover change in China's metropolises over the last three decades. *Environmental Monitoring and Assessment* **179**: 1–14. DOI:10.1007/s10661-010-1715-x.

Tilman D. 1999. Global environmental impacts of agricultural expansion: the need for sustainable and efficient practices. *Proceedings of the National Academy of Sciences* **96**: 5995–6000. DOI:10.1073/pnas.96.11.5995.

Tomczak M. 1998. Spatial interpolation and its uncertainty using automated anisotropic inverse distance weighting (IDW)-cross-validation/jacknife approach. *Journal of Geographic Information and Decision Analysis* **2**: 18–30.

Toms JD, Lesperance ML. 2003. Piecewise regression: a tool for identifying ecological thresholds. *Ecology* **84**: 2034–2041.

Wang X, Li L. 2007. The drying-up of the Western Liaohe River and the countermeasures to the problem. *Journal of Arid Land Resources and Environment* **6**: 79–83(in Chinese with English abstract).

Wang J, Rich PM, Price KP. 2003. Temporal responses of NDVI to precipitation and temperature in the central Great Plains, USA. *International Journal of Remote Sensing* **24**: 2345–2364. DOI:10.1080/01431160210154812.

Wang F, Wang X, Zhao Y, Yang Z. 2013. Correlation analysis of NDVI dynamics and hydro-meteorological variables in growth period for four land use types of a water scarce area. *Earth Science Informatics* **7**: 187–196. DOI:10.1007/s12145-013-0139-x.

Wu D, Zhao X, Liang S, Zhou T, Huang K, Tang B, Zhao W. 2015. Time-lag effects of global vegetation responses to climate change. *Global Change Biology* **21**: 3520–3531. DOI:10.1111/gcb.12945.

Yong B, Ren L, Hong Y, Gourley JJ, Chen X, Dong J, Wang W, Shen Y, Hardy J. 2013. Spatial–temporal changes of water resources in a typical semiarid basin of North China over the past 50 years and assessment of possible natural and socioeconomic causes. *Journal of Hydrometeorology* **14**: 1009–1034. DOI:10.1175/JHM-D-12-0116.1.

Yuan W, Liu D, Dong W, Liu S, Zhou G, Yu G, Zhao T, Feng J, Ma Z, Chen J, Chen Y, Chen S, Han S, Huang J, Li L, Liu H, Liu S, Ma M, Wang Y, Xia J, Xu W, Zhang Q, Zhao X, Zhao L. 2014. Multiyear precipitation reduction strongly decreases carbon uptake over northern China. *Journal of Geophysical Research, Biogeosciences* **119**: 8–16. DOI:10.1002/2014jg002608.

Zeng F, Collatz G, Pinzon JE, Ivanoff A. 2013. Evaluating and quantifying the climate-driven interannual variability in Global Inventory Modeling and Mapping Studies (GIMMS) Normalized Difference Vegetation Index (NDVI3g) at global scales. *Remote Sensing* **5**: 3918–3950. DOI:10.3390/rs5083918.

Zhang Z, Wang X, Zhao X, Liu B, Yi L, Zuo L, Wen Q, Liu F, Xu J, Hu S. 2014. A 2010 update of National Land Use/Cover Database of China at 1: 100000 scale using medium spatial resolution satellite images. *Remote Sensing of Environment* **149**: 142–154. DOI:10.1016/j.rse.2014.04.004.

Zhao M, Running SW. 2010. Drought-induced reduction in global terrestrial net primary production from 2000 through 2009. *Science* **329**: 940–943. DOI:10.1126/science.1192666.

Zhou L, Tucker CJ, Kaufmann RK, Slayback D, Shabanov NV, Myneni RB. 2001. Variations in northern vegetation activity inferred from satellite data of vegetation index during 1981 to 1999. *Journal of Geophysical Research* **106**: 20069–20083. DOI:10.1029/2000JD000115.

